Journal of Magnetic Resonance **143,** 39–44 (2000)
doi:10.1006/jmre.1999.1948, available online at http://www.idealibrary.com on IDEAL®

^{17}O-Decoupled ^{1}H Spectroscopy and Imaging with a Surface Coil: STEAM Decoupling

Sridhar R. Charagundla, Umamaheswar Duvvuri, Elizabeth A. Noyszewski, Rahul Dandora, Alan H. Stolpen, J. S. Leigh, and Ravinder Reddy

Department of Radiology, University of Pennsylvania, Philadelphia, Pennsylvania 19104

Received April 26, 1999; revised September 30, 1999

^{17}O-decoupled ^{1}H spin-echo imaging has been reported as a means of indirect ^{17}O detection, with potential application to measurement of blood flow and metabolism. In its current form, ^{17}O decoupling requires large RF amplitudes and a 180° refocusing pulse, complicating its application in volume and surface coils, respectively. To overcome this problem, we have developed an ^{17}O-decoupled proton stimulated echo sequence ("STEAM decoupling") to allow ^{17}O detection with a surface coil. A high B_1 amplitude is easily generated, allowing complete decoupling of ^{17}O and ^{1}H. Slice-selective, ^{17}O-decoupled ^{1}H imaging is readily performed and the sequence is easily adapted for localized spectroscopy. Intrinsic correction for variations in B_1 and further compensation for B_1 inhomogeneity are discussed. © 2000 Academic Press

Key Words: **^{17}O; decoupling; stimulated echo; surface coil.**

INTRODUCTION

Techniques for NMR detection of ^{17}O have continued to progress toward clinical feasibility, approaching adequate sensitivity and specificity for use *in vivo.* The ultimate goal of these technique-development efforts is compelling: conversion of $^{17}O_2$ to $H_2{}^{17}O$ may be monitored directly, providing a potentially unambiguous measure of oxidative metabolic rate (*1–9*). While the physical basis for most ^{17}O detection techniques has been established for over 20 years (*10*), these principles have only recently been applied to proton MRI, resulting in a host of so-called "indirect" ^{17}O detection methods, whereby ^{17}O concentration is ascertained through changes in the proton NMR signal (*7, 11–13*). In particular, the development of ^{17}O-decoupled proton spectroscopy has been met with enthusiasm; $H_2{}^{17}O$ concentration is calculated by measuring the effect of ^{17}O decoupling on the evolution of a proton spin-echo (*11*). This method has been used for imaging $H_2{}^{17}O$ distribution in tissue phantoms and animals (*8, 13, 14*).

However, use of ^{17}O-decoupled proton MR in its current form is limited by several considerations. First, ^{17}O decoupling as it is currently done requires a proton π refocusing pulse; generating a spin echo in this manner requires sufficient RF homogeneity, which can be obtained only in a volume coil. However, ^{17}O decoupling requires substantial RF power for adequate sensitivity. Previous work has shown that decoupling efficiency is optimal for a B_1 of at least 2.6 to 3.5 G ($\omega_1 = 1.5$ to 2 kHz) for ^{17}O concentrations less than 1.4 atom% (*8, 13*). This high RF amplitude would clearly be difficult to obtain in large volume coils such as those used in clinical MRI. Finally, signal-to-noise ratio is of paramount importance to indirect ^{17}O detection *in vivo,* and use of a volume coil offers suboptimal sensitivity to the NMR signal (*15*) and lower filling factors.

In this article, we present a method for performing ^{17}O-decoupled ^{1}H spectroscopy and imaging using a double-tuned surface coil. By applying ^{17}O-decoupling pulses during a proton stimulated echo sequence ("STEAM decoupling"), we are able to reduce or eliminate ^{17}O-mediated proton T_2 relaxation, in exact analogy to ^{17}O decoupling during a spin echo (*8, 11, 13*). By comparing proton stimulated echo signal intensity with and without ^{17}O decoupling, we can quantify ^{17}O concentration. We also demonstrate that STEAM decoupling is readily adapted for indirect ^{17}O imaging and discuss its potential in localized spectroscopy as well.

THEORY

In studying the pH dependence of water proton T_2 relaxation times, Meiboom determined that the spin-5/2 nucleus ^{17}O was an important contributor to proton transverse relaxation (*10*). When bound in $H_2{}^{17}O$, ^{1}H and ^{17}O exhibit scalar coupling ($J =$ 90 Hz) (*16*). This interaction is modulated by chemical exchange of protons between water molecules and by rapid longitudinal relaxation of ^{17}O. As a result, water proton T_2 times are shortened by ^{17}O, according to a standard formula for relaxivity:

$$\frac{1}{T_2} = \frac{1}{T_2^0} + R_2 f, \qquad [1]$$

where T_2 represents the proton transverse relaxation time, T_2^0 is the proton T_2 in the absence of ^{17}O, R_2 is the T_2 relaxivity of ^{17}O, and f is the ^{17}O atom fraction (0.037 atom% is natural abundance, about 20 mM in pure water). ^{17}O relaxivity is

1090-7807/00 $35.00

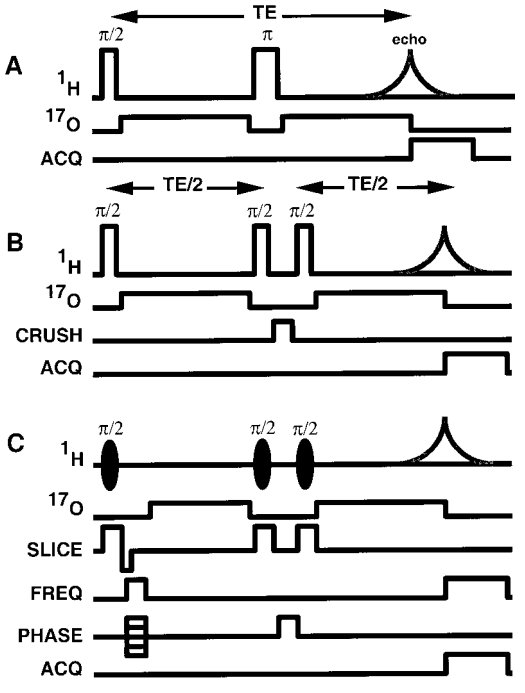

FIG. 1. Pulse sequence diagrams for ^{17}O measurement using conventional and STEAM decoupling: (A) proton spin-echo sequence previously used for ^{17}O-decoupled spectroscopy. Irradiation of the ^{17}O resonance during the evolution time prolongs the proton T_2 in a ^{17}O-concentration-dependent manner; (B) proton stimulated echo with ^{17}O decoupling pulses (STEAM decoupling). ^{17}O decoupling pulses are applied during the evolution time where proton relaxation is governed by T_2; (C) ^{17}O-decoupled proton stimulated echo imaging. ^{17}O decoupling pulses are applied when gradients are off, to prevent off-resonance effects. In general, long TEs are required for adequate ^{17}O sensitivity.

maximized in water at neutral pH; deviations from neutral pH increase the proton exchange time (by base or acid catalysis) and reduce the relaxivity of ^{17}O. On the other hand, shortening ^{17}O T_1 also reduces ^{17}O relaxivity. In effect, this can be accomplished by irradiating the ^{17}O nucleus with a decoupling pulse at the ^{17}O Larmor frequency. The application of a decoupling pulse essentially removes any effect ^{17}O may have on proton transverse relaxation, increasing proton T_2 to T_2^0. This has traditionally been done by applying ^{17}O decoupling pulses during the evolution time of a proton spin echo, as shown in Fig. 1A (*11*). Using this sequence, the proton signal can be calculated as (*8*)

$$S_0 = S \exp\left[-\mathrm{TE} \times \left(\frac{1}{T_2^0} + R_2 f \right) \right]$$

$$S_{\mathrm{DC}} = S \exp\left[-\mathrm{TE} \times \left(\frac{1}{T_2^0} + R_2 f \cdot \{1 - d\} \right) \right], \qquad [2]$$

where S_{DC} and S_0 represent the proton signal intensities for a spin echo of echo time TE with and without decoupling, respectively, and d represents the decoupling "efficiency" (ranging from 0 to 1). ^{17}O concentration is calculated from proton signal enhancement by (*8*)

$$f = \frac{\ln\left(\frac{S_{\mathrm{DC}}}{S_0} \right)}{\mathrm{TE} \cdot R_2 \cdot d}. \qquad [3]$$

Typically, the optimal decoupling power for measuring ^{17}O concentration is determined empirically. Decoupling power is increased until proton signal enhancement reaches a plateau, and this power level is assumed to be sufficient for complete decoupling of ^{17}O from ^{1}H.

In order to perform ^{17}O detection with a surface coil, it is necessary to circumvent the need for a 180° refocusing pulse. This is possible by applying decoupling pulses during, for example, a three-pulse stimulated echo sequence, as shown in Fig. 1B. The important feature of the decoupling pulses is that they be applied while proton T_2 relaxation is occurring. In a stimulated echo sequence, T_2 relaxation occurs between pulses 1 and 2 and after pulse 3. By irradiating ^{17}O at these times, we can eliminate ^{17}O as a proton T_2 relaxation pathway and calculate ^{17}O concentration.

However, the B_1 inhomogeneity intrinsic to a surface coil implies a nonuniform decoupling efficiency over the sample volume. Therefore, by Eq. [3], the calculated ^{17}O concentration is potentially susceptible to changes in RF intensity. It is possible to deal with this source of error by noting that decoupling efficiency is essentially one for powers above some threshold value (*13*). By applying a decoupling power beyond this level, high decoupling efficiency can be obtained for a large portion of the sample.

Slice-selective ^{17}O-decoupled ^{1}H imaging can be performed by converting the square RF pulses of the stimulated echo sequence to sinc pulses during slice-select gradients, as in Fig. 1C. This can be further modified for localized spectroscopy by applying the slice-select gradients along three orthogonal directions (*17*). ^{17}O was not irradiated during the application of imaging gradients to avoid off-resonance decoupling effects (*13*). In all pulse sequences, both imaging and spectroscopic, ^{17}O irradiation was turned off during proton signal acquisition (see Fig. 1); this meant that the linewidth of the actual acquired proton signal was unchanged by the application of ^{17}O decoupling during the pulse sequence.

METHODS

Experiments were performed on a 2-T whole body superconducting magnet interfaced to a custom-built NMR spectrometer. A 3-cm-diameter surface coil was double-tuned to the ^{17}O and ^{1}H Larmor frequencies (11.7 and 86.1 MHz, respectively) according to the method of Schnall *et al.* (*18*) and placed in a gradient insert capable of 2.3 G/cm. In all experiments, B_1 was calibrated by determining the RF pulse width

generating maximum signal amplitude; this "nominal" $\pi/2$ pulse was used to calculate the effective B_1 of the excited volume. Animal experiments were performed on male Sprague–Dawley rats weighing approximately 300–400 g. Rats were anesthetized using intramuscular injections of a ketamine/xylazine mixture.

The pulse sequence shown in Fig. 1B was applied to a spherical 10-ml water phantom containing natural abundance $H_2{}^{17}O$ in phosphate-buffered saline (PBS) placed on the surface coil, in order to determine the decoupling power (B_1) generating maximum proton signal enhancement. Proton spectra for decoupling powers varying from 0 to 2.2 kHz were collected with a TR of 15 s, TE of 600 and 1300 ms, and 2048 points at 5 kHz bandwidth. To demonstrate ^{17}O imaging, the surface coil was used to image a cylindrical phantom containing three 5-mm-diameter borosilicate tubes, each containing 200 μl of water enriched with $H_2{}^{17}O$. The concentrations were 0.037 (natural abundance), 0.2, and 0.5 atom%. The tubes were immersed in water to minimize susceptibility artifacts. Imaging parameters were TR of 10 s, TE of 600 ms, FOV of approximately 2 cm with 5 kHz bandwidth, slice thickness of approximately 5 mm, and a 256 by 128 acquisition matrix. For the decoupled image, decoupling power was 2.5 kHz.

STEAM decoupling was also used for *in vivo* ^{17}O detection. The sequence for STEAM decoupled spectroscopy (Fig. 1B) was applied to rat brain containing natural abundance $H_2{}^{17}O$; proton spectra from rat brain were collected with a TR of 5 s, TE of 200 ms, and 1024 points at 5 kHz bandwidth. Finally, the sequence was applied to the calf of a human volunteer; proton spectra were acquired with TR of 8 s, TE of 40 ms, and 1024 points at 5 kHz bandwidth. In each case, decoupling power was approximately 1 kHz, and a crusher gradient as shown in Fig. 1B was necessary to eliminate transverse magnetization created by the second $\pi/2$ pulse.

RESULTS

Efforts to calibrate the surface coil on a PBS phantom yielded the data shown in Fig. 2. Proton signal enhancement was greatest for a B_1 beyond 1 kHz. The profile of the curve is similar to that of previous decoupling experiments with a double-tuned volume coil (*13*), with a steep increase in proton signal enhancement as B_1 approaches 1 kHz and a plateau occurring beyond 1 kHz. Figure 3 shows slice-selective images of three tubes with different $H_2{}^{17}O$ concentrations. The surface coil was located near the bottom of the tubes; the imaged slice was parallel to the plane of the coil. For subsequent *in vivo* experiments, a decoupling power of approximately 1 kHz was utilized.

Application of STEAM decoupling for *in vivo* ^{17}O detection followed. Stimulated echo proton spectra of rat brain collected with and without ^{17}O decoupling are displayed in Fig. 4. The signal enhancement with decoupling was approximately 12%, which is in good agreement with signal enhancement obtained

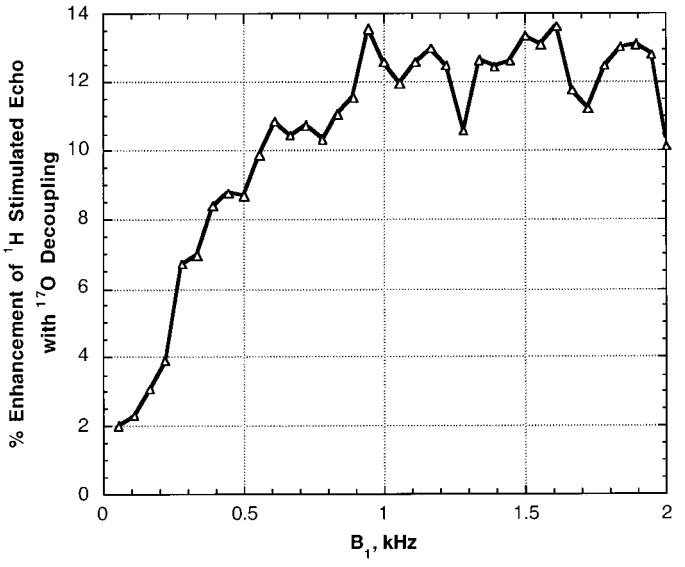

FIG. 2. Graph of proton stimulated echo signal enhancement as a function of decoupling power. Data were collected on a spherical water phantom with a TR of 15 s (30 s per decoupled/nondecoupled pair), TE of 600 ms, and 2048 points at 5 kHz bandwidth. Once adequate decoupling power is achieved, the signal enhancement reaches a plateau. Choosing a decoupling power well above the "threshold" value ensures high decoupling efficiency even with substantial B_1 fall off.

using volume coils on natural abundance water phantoms (data not shown). Finally, the STEAM decoupling sequence and surface coil were used to detect ^{17}O in the human calf. Decoupled and nondecoupled spectra are shown in Fig. 5. The water peak of the proton spectrum shows a signal enhancement of 8%, while the fat peak shows exceedingly small, insignificant enhancement (0.06%).

DISCUSSION

The performance of the double-tuned surface coil was similar to that of the double-tuned volume coil in several respects. The decoupling calibration curve (Fig. 2) shows that at low decoupling powers, ^{17}O persists as a T_2 relaxation pathway for ^{1}H, but that as decoupling power is increased, ^{17}O contributes less to ^{1}H relaxation, causing a lengthening of proton T_2 and a corresponding narrowing of the proton resonance. At sufficiently high decoupling powers, the proton signal enhancement due to T_2 prolongation reaches a plateau, indicating complete ^{17}O decoupling. Once this level is reached, proton signal enhancement can be reliably used to calculate ^{17}O concentration. The surface coil exhibited complete decoupling at a B_1 beyond approximately 1 kHz, which is in good agreement with previous estimates of decoupling power requirements (*8, 13*).

While this power level has been shown to comply with SAR limitations (*13*), it may be difficult to achieve sufficient power for complete decoupling with standard clinical volume coils, such as head or body coils. If complete decoupling is not

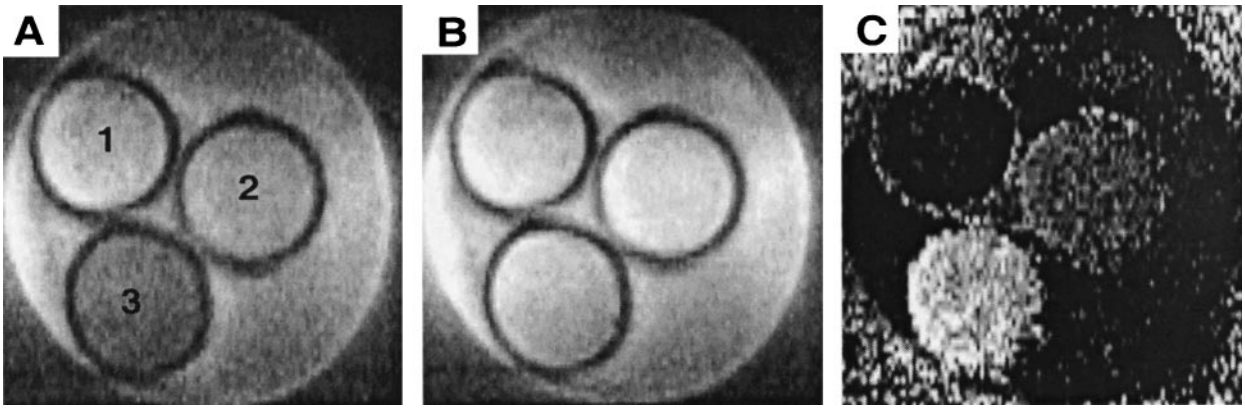

FIG. 3. STEAM decoupled imaging of three tubes containing different concentrations of $H_2{}^{17}O$. Tubes 1, 2, and 3 contain natural abundance (0.037), 0.2, and 0.5 atom% $H_2{}^{17}O$. Imaging plane was approximately 1.5 cm above and parallel to the plane of the surface coil: (A) nondecoupled image. T_2 contrast, due to variations in ^{17}O concentration, is evident; (B) decoupled image. T_2 contrast is markedly diminished; ^{17}O decoupling has virtually eliminated ^{17}O as a T_2-relaxation pathway for ^1H; (C) ratio of images (A) and (B). ^{17}O quantification is possible with the ratio image, and exhibits fewer artifacts than images (A) or (B). Imaging parameters were TR = 10 s, TE = 600 ms, 2 cm FOV, 5 kHz bandwidth, 5-mm slice thickness, and a 256 × 128 acquisition matrix; decoupling power was 2.5 kHz.

achieved, calculations of ^{17}O concentration are susceptible to variations in B_1 due to coil inhomogeneities or other instrumental imperfections. Low decoupling efficiencies also compromise the overall sensitivity to ^{17}O. In these situations, a surface coil would be a useful substitute for the purposes of localized spectroscopy or imaging.

Effects of B_1 inhomogeneity are evident to some degree in surface coil images of phantoms with different ^{17}O concentrations (Fig. 3). B_0 inhomogeneities may have produced some of the spatial differences in signal intensity, but this was likely to be small compared to the effect of B_1 inhomogeneity because (1) susceptibility mismatch was minimized by immersing the tubes in water, and (2) the spectroscopic linewidth of the whole phantom was small—consider a small sample in a large-bore magnet. In any case, heterogeneity in image intensity is clearly visible in Figs. 3A and 3B, but the ratio image (Fig. 3C) is relatively free of such artifacts. In the process of generating the ratio image, artifacts common to both decoupled and nondecoupled images may potentially be canceled out. This demonstrates the concept of the decoupled image as an experimental control, allowing correction of ^{17}O images for variations in B_1. Ratio imaging may even correct for variations in water content and evolving tissue pathology, improving the specificity of STEAM decoupling for ^{17}O. Further compensation for B_1 inhomogeneity can be achieved with the use of selective adiabatic pulses in place of the sinc pulses depicted in Fig. 1 (*19, 20*).

In Fig. 5, comparison of the nondecoupled and decoupled proton spectra of human calf demonstrates ^{17}O detection in humans *in vivo*. The enhancement of the water peak (8%) upon decoupling indicates the presence of natural abundance $H_2{}^{17}O$. We attribute the lack of lipid signal enhancement to the fact that lipid protons are not scalar coupled to oxygen atoms and are not undergoing rapid chemical exchange. The lipid resonance could provide an internal control during *in vivo* localized spectroscopy experiments, allowing adjustment for changes in B_1 and other experimental variables. The enhancement of the water peak *in vivo* was lower than that obtained for natural abundance water phantoms, due to the presence of buffers which catalyze proton exchange and reduce ^{17}O relaxivity (*8*). Since the major source of the water peak is calf muscle parenchyma, these results suggest that STEAM decoupling can be used to monitor oxidative metabolism in exercising or ischemic muscle. The fat peak is more intense than the water peak because the RF penetration from the surface coil was fairly superficial, and the excited volume consisted of a large

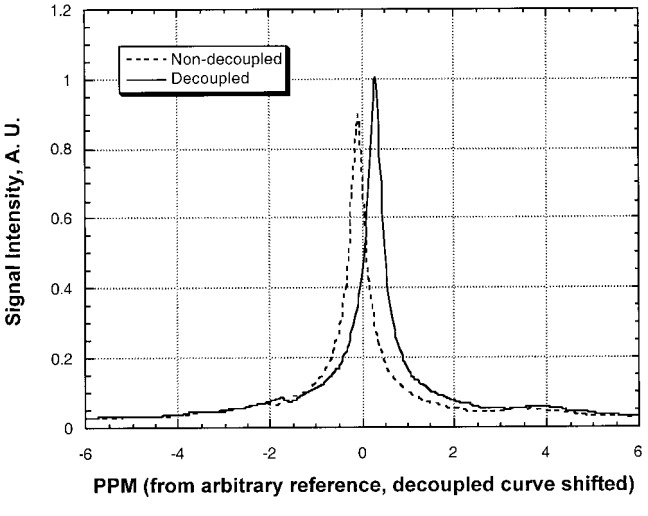

FIG. 4. *In vivo* ^1H spectra of rat brain collected with STEAM decoupled spectroscopy. TR was 5 s (requiring 10 s for a decoupled/nondecoupled pair), TE was 200 ms, and 1024 points were collected at 5 kHz bandwidth. A 12% enhancement was obtained for the water peak upon decoupling, indicating the presence of natural abundance $H_2{}^{17}O$.

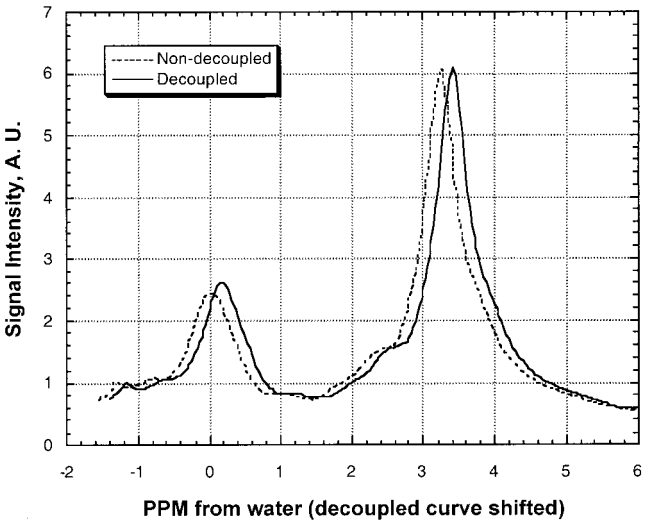

FIG. 5. *In vivo* ^{1}H spectra of human calf muscle collected with STEAM decoupled spectroscopy. Spectra were collected with a TR of 8 s, TE of 40 ms, and 1024 points at 5 kHz bandwidth. The water peak underwent an 8% enhancement, while the lipid peak showed almost no enhancement with decoupling. Protons in fat are not undergoing rapid chemical exchange with water; ^{17}O in water does not contribute to their relaxation and ^{17}O decoupling should produce no enhancement, as shown.

amount of subcutaneous and muscular fat along with a smaller amount of muscle water. These spectra were not localized, and therefore no particular slice was selected.

Localized *in vivo* measurements of ^{17}O may be best accomplished by modifying the sequence in Fig. 1C for single-voxel or Hadamard spectroscopy. An advantage of using localized excitation is that B_1 tends to be homogeneous within a small voxel, facilitating the calibration of decoupling power. In other words, the pulse sequence in Fig. 1B can be modified to obtain data similar to those in Fig. 2, but for a single voxel, thereby assuring complete decoupling throughout the voxel.

It is interesting to note that the proton signal enhancements obtained with ^{17}O decoupling *in vivo* differ from those predicted by previously published values for R_2 *in vitro* (*9, 10*). These results suggest a different value for R_2 *in vivo;* measurement of this parameter is a subject of our continued investigation. However, ^{17}O quantification can be corrected for variations in R_2 by using a sample of known ^{17}O concentration (e.g., natural abundance) as a reference.

Using a surface coil which is double-tuned to the ^{1}H and ^{17}O Larmor frequencies carries several advantages over orthogonal coil setups, as has been presented earlier (*13*). In addition to the ease of calibrating B_1 and matching B_1 profiles at both frequencies, the double-tuned feature greatly facilitates the construction of the surface coil. As demonstrated by the variety of experiments in this paper, the coil is versatile and convenient. With no modification, the coil was used for studies of phantoms, animals, and humans and performed adequately in all situations. Finally, improvements in proton signal-to-noise ratio translate into improved accuracy in ^{17}O quantification (*8*), and this is of paramount importance in the study of perfusion and metabolism with ^{17}O. Since surface coils are superior to volume coils in terms of sensitivity to the NMR signal, their use for ^{17}O detection may considerably improve the measurement of physiological parameters *in vivo.*

^{17}O can also be quantified indirectly with $T_{1\rho}$-dispersion proton MRI, a technique which does not require irradiation of the ^{17}O nucleus and may therefore be used on a clinical scanner without hardware modification (*7, 9*). $T_{1\rho}$-dispersion imaging calculates ^{17}O concentration by using spin-locking pulses to generate ^{17}O-based contrast. Many analogies exist between ^{17}O-decoupled and $T_{1\rho}$-dispersion MRI, including the use of control images (where ^{17}O has no effect on proton relaxation) and ratio images. It is possible that with a strategy similar to the one presented here, $T_{1\rho}$-dispersion MRI may also be performed using a surface coil.

In conclusion, we have developed a pulse sequence based on the stimulated echo that allows ^{17}O detection *in vivo* through the use of a double-tuned surface coil. Its performance is similar to that of a double-tuned volume coil, but does not require a refocusing pulse and is easily adapted for use in phantoms, animals, or humans. Given its small size, it can easily produce sufficient RF power for complete ^{17}O decoupling and is readily utilized for localized spectroscopy and imaging. Careful choice of a decoupling power can reduce the effects of B_1 inhomogeneity on ^{17}O quantification, although we are investigating other strategies to remove this effect altogether. Experiments using STEAM decoupling to measure cerebral blood flow and oxygen consumption are in progress.

ACKNOWLEDGMENTS

This work was supported by NIH Grants RR02305 and R29-NS35625 and by a grant from the Whitaker foundation. S. R. C. is an MSTP trainee (Grant 5T32-GM07170). U. D. is supported by NIH Grant MH1196-O1A1.

REFERENCES

1. T. Arai, S. Nakao, K. Mori, K. Ishimori, I. Morishima, T. Miyazawa, and B. Fritz-Zieroth, *Biochem. Biophys. Res. Commun.* **169,** 153–158 (1990).
2. T. Arai, K. Mori, S. Nakao, K. Watanabe, K. Kito, M. Aoki, H. Mori, S. Morikawa, and T. Inubushi, *Biochem. Biophys. Res. Commun.* **179,** 954–961 (1991).
3. J. Pekar, L. Ligeti, Z. Ruttner, R. C. Lyon, T. M. Sinnwell, P. van Gelderen, D. Fiat, C. T. Moonen, and A. C. McLaughlin, *Magn. Reson. Med.* **21,** 313–319 (1991).
4. J. Pekar, T. Sinnwell, L. Ligeti, A. S. Chesnick, J. A. Frank, and A. C. McLaughlin, *J. Cereb. Blood Flow Metab.* **15,** 312–320 (1995).
5. D. Fiat, and S. Kang, *Neurol. Res.* **14,** 303–311 (1992).
6. D. Fiat, L. Ligeti, R. C. Lyon, Z. Ruttner, J. Pekar, C. T. Moonen, and A. C. McLaughlin, *Magn. Reson. Med.* **24,** 370–374 (1992).
7. S. R. Charagundla, A. H. Stolpen, J. S. Leigh, and R. Reddy, *Magn. Reson. Med.* **39,** 588–595 (1998).
8. A. H. Stolpen, R. Reddy, and J. S. Leigh, *J. Magn. Reson.* **125,** 1–7 (1997).

9. R. Reddy, A. H. Stolpen, and J. S. Leigh, *J. Magn. Reson. B* **108,** 276–279 (1995).

10. S. Meiboom, *J. Chem. Phys.* **34,** 375–388 (1961).

11. I. Ronen, and G. Navon, *Magn. Reson. Med.* **32,** 789–793 (1994).

12. A. L. Hopkins, and R. G. Barr, *Magn. Reson. Med.* **4,** 399–403 (1987).

13. R. Reddy, A. H. Stolpen, S. R. Charagundla, E. K. Insko, and J. S. Leigh, *Magn. Reson. Imaging* **14,** 1073–1078 (1996).

14. I. Ronen, J. H. Lee, H. Merkle, K. Ugurbil, and G. Navon, *NMR Biomed.* **10,** 333–340 (1997).

15. C.-N. Chen, and D. I. Hoult, "Biomedical Magnetic Resonance Technology," IOP Publishing, New York (1989).

16. L. J. Burnett, and A. H. Zeltmann, *J. Chem. Phys.* **60,** 4636–4637 (1974).

17. J. Frahm, K. D. Merboldt, W. Hanicke, and A. Haase, *J. Magn. Reson.* **64,** 81–93 (1985).

18. M. D. Schnall, V. Harihara Subramanian, J. S. Leigh, Jr., and B. Chance, *J. Magn. Reson.* **65,** 122–129 (1985).

19. S. Conolly, D. Nishimura, and A. Macovski, *J. Magn. Reson.* **83,** 324–334 (1989).

20. M. Zweckstetter, and T. A. Holak, *J. Magn. Reson.* **133,** 134–147 (1998).